

MORPHOLOGICAL STUDY OF THE PARANASAL SINUSES USING MULTIDETECTOR COMPUTED TOMOGRAPHY AND ITS CLINICAL APPLICATIONS IN PLANNING ENDOSCOPIC SINUS SURGERY PROCEDURE IN UTTAR PRADESH, INDIA

Abuzar Abdalla¹, Danish Anwer^{2*}, Tagreed Ahmed³, Muntaser Mohammed Fadoul Alhassen⁴, Hamid Ansari⁵

^{1,2,3}Assistant Professor, Department of Human Anatomy, College of Medicine, Jazan University, Jazan, Saudi Arabia

⁴Lecturer, Dept of Diagnostic Radiology, College of Applied Medical Science, Jazan University

⁵Associate Professor, Autonomous State Medical College, Kanpur Dehat, Uttar Pradesh, India

*Corresponding Author: Dr. Danish Anwer (Email: dr.danish07@gmail.com).

ABSTRACT

Background and Introduction: The paranasal sinuses exhibit considerable anatomical variability that carries direct implications for the safety and success of functional endoscopic sinus surgery (FESS). Preoperative multidetector computed tomography (MDCT) remains the gold standard for identifying sinonasal anatomical variations, assessing disease severity, and guiding individualized surgical planning. Despite the clinical importance of this data, region-specific normative and variation-prevalence information from central India remains limited, creating a significant evidence gap for surgeons practicing in this population.

Methods: A descriptive, observational, cross-sectional study was conducted over twelve months from January 2025 to December 2025 at the Department of Anatomy in collaboration with the Department of Radiology and Imaging, Autonomous State Medical College, Kanpur Dehat, Uttar Pradesh. A total of 50 adult MDCT scans of the paranasal sinuses were evaluated using multiplanar coronal, axial, and sagittal reconstructions. Anatomical variations, sinus dimensions, Keros classification of olfactory fossa depth, and Lund-Mackay disease severity scores were systematically documented using a predesigned proforma. Data were analyzed using IBM SPSS version 23 with descriptive statistics, chi-square testing, and Pearson's correlation coefficient.

Results: Nasal septal deviation was the most prevalent variation, identified in 62.0 percent of participants, followed by agger nasi cells (54.0%), concha bullosa (42.0%), enlarged inferior turbinate (34.0%), and Haller cells (26.0%). Onodi cells were present in 20.0 percent of cases. Keros Type II olfactory fossa depth was the most common configuration (52.0%), while the surgically high-risk Keros Type III was found in 18.0 percent of participants. Lund-Mackay scoring revealed moderate sinusitis as the predominant disease category (46.0%), with a statistically significant association between anatomical variations and greater disease severity ($p = 0.006$). Maxillary and frontal sinus dimensions showed statistically significant gender-based differences, with males recording larger measurements.

Conclusion: This study provides clinically relevant, region-specific MDCT data on paranasal sinus morphology and anatomical variations from central India, documenting a high prevalence of surgically significant variants. The findings support the mandatory use of structured preoperative MDCT evaluation incorporating Keros classification and Lund-Mackay scoring to improve surgical safety and outcomes in patients undergoing endoscopic sinus surgery.

KEYWORDS: Paranasal sinus anatomy, multidetector computed tomography, endoscopic sinus surgery, anatomical Variations, ostiomeatal complex

INTRODUCTION

The paranasal sinuses are a complex system of air-filled cavities located within the bones of the skull and face, communicating with the nasal cavity through narrow ostia and drainage pathways. These structures, which include the maxillary, frontal, ethmoid, and sphenoid sinuses, are developmentally, anatomically, and clinically interrelated in ways that make their detailed understanding indispensable for surgeons, radiologists, and anatomists alike. The emergence of functional endoscopic sinus surgery (FESS) as the standard surgical approach for managing chronic rhinosinusitis and related sinus pathologies has transformed the clinical importance of paranasal sinus anatomy, elevating it from a largely academic subject to one with immediate operative implications (Stammler & Kennedy, 1995).

Chronic rhinosinusitis is one of the most prevalent inflammatory conditions affecting the upper respiratory tract, imposing a significant burden on quality of life and healthcare systems globally. In India, the condition is compounded by environmental factors including air pollution, dust exposure, and a high prevalence of allergic rhinitis, making it a frequently encountered condition in both outpatient and surgical settings. Surgical management through FESS aims to restore normal mucociliary drainage by widening the natural ostia of the sinuses, particularly targeting the ostiomeatal complex (OMC), which serves as the critical drainage pathway for the anterior group of sinuses (Laine & Smoker, 1992). The success and safety of this procedure are fundamentally dependent on the surgeon's preoperative knowledge of the

patient's unique sinus anatomy, since the region is immediately adjacent to vital structures including the orbit, the optic nerve, the internal carotid artery, the cribriform plate, and the anterior skull base.

Anatomical variations in the paranasal sinus region are not exceptions — they are the rule. Bolger et al. (1991), in a landmark study, systematically catalogued bony anatomical variations in the sinonasal region using computed tomography (CT) and demonstrated that the vast majority of individuals carry at least one clinically significant variation that could influence surgical planning or risk. These variations include a deviated nasal septum, concha bullosa (pneumatization of the middle turbinate), paradoxically bent middle turbinate, Haller cells (infraorbital ethmoid cells), Onodi cells (sphenoidal cells adjacent to the optic nerve), agger nasi cells, and hypoplasia or aplasia of individual sinuses. Each of these has a direct bearing on the surgical approach, the instruments used, and the likelihood of encountering complications (Earwaker, 1993).

The ostiomeatal complex deserves particular attention. This functional unit, comprising the maxillary sinus ostium, the infundibulum, the hiatus semilunaris, the ethmoid bulla, and the middle meatus, represents the final common drainage pathway for the maxillary, anterior ethmoid, and frontal sinuses. Obstruction at any point in this pathway can trigger a cascade of mucosal disease extending to all three sinus groups. Anatomical variants that narrow or obstruct the OMC, such as a large agger nasi cell or an extensively pneumatized concha bullosa, are therefore mechanistically linked to chronic sinusitis and must be identified and documented before surgery (Zinreich, 1998). Failure to recognize an Onodi cell, for example, has been directly implicated in cases of inadvertent optic nerve injury during sphenoid or posterior ethmoid dissection, one of the most dreaded complications in sinus surgery (Kantarci et al., 2004).

Multidetector computed tomography (MDCT) has emerged as the imaging modality of choice for preoperative evaluation of the paranasal sinuses. Compared to conventional CT, MDCT offers superior spatial resolution, faster acquisition times, isotropic voxel data allowing reconstruction in any plane without loss of quality, and the capability for three-dimensional volume rendering. Coronal reconstruction remains the standard plane for sinonasal evaluation because it best mirrors the anatomical perspective encountered during endoscopic surgery and provides the clearest depiction of the OMC, the lamina papyracea, the cribriform plate, and the relationships between ethmoid cells (Rao & el-Noueam, 1998). Axial and sagittal reformats complement coronal views by clarifying the anteroposterior extent of disease, the depth of the olfactory fossa, and the sphenoid sinus relationships with the optic canal and carotid groove.

Despite international literature richly documenting paranasal sinus variations using CT, Indian data remain comparatively sparse, particularly from smaller medical institutions serving semi-urban and rural populations in states like Uttar Pradesh. Studies from South India and metropolitan centers have begun to address this gap, but regional normative data from central India are still limited (Kaygusuz et al., 2013; Fadda et al., 2012). This matters because the prevalence and type of anatomical variations can differ meaningfully across ethnic and geographic groups, and surgical planning that relies exclusively on Western or metropolitan normative databases may not optimally serve the local patient population.

Nouraei et al. (2009) demonstrated that specific anatomical variations, including a low-lying cribriform plate, Onodi cells, and dehiscence of the carotid canal within the sphenoid, substantially elevated operative risk during ESS, and emphasized that radiological assessment should be mandatory and standardized before any surgical intervention. Similarly, Laine and Smoker (1992) showed that surgeons who reviewed coronal CT images preoperatively had significantly lower rates of major intraoperative complications compared to those who operated without such review.

The present study was therefore designed to systematically document and analyze the morphological characteristics and anatomical variations of the paranasal sinuses in patients referred for CT imaging at Autonomous State Medical College, Kanpur Dehat, using MDCT as the primary investigative tool. The findings are intended to generate region-specific data on variation prevalence, to correlate anatomical patterns with clinical presentations of sinusitis, and to provide a radiological reference that can assist surgeons in safer and more precise preoperative planning for endoscopic sinus surgery.

This study aimed to evaluate and document the morphological characteristics and anatomical variations of the paranasal sinuses using multidetector computed tomography (MDCT), and to assess their clinical significance and relevance in preoperative planning for endoscopic sinus surgery.

METHODOLOGY

Study Design

This study was conducted as observational cross-sectional study.

Study Site

The study was carried out in the Department of Anatomy in collaboration with the Department of Radiology and Imaging at Autonomous State Medical College, Kanpur Dehat, Uttar Pradesh.

Study Duration

The study was conducted over a period of twelve months, from January 2025 to December 2025.

Sampling and Sample Size

Purposive sampling was employed to recruit adult patients who had been referred for CT paranasal sinus evaluation at the study site during the study period. A total of 50 MDCT scans were included in the final analysis. Both male and female patients were included to allow gender-based comparisons of sinus dimensions and variation frequencies. Age was recorded from clinical records for each participant, with only adults aged 18 years and above considered for inclusion.

This sample size is consistent with those of comparable observational radiological studies on paranasal sinus anatomy reported in the literature (Kantarci et al., 2004; Fadda et al., 2012).

Inclusion and Exclusion Criteria

Patients aged 18 years and above of either gender who underwent MDCT of the paranasal sinuses for clinical indications during the study period and provided informed consent for inclusion of their imaging data were included in the study. Scans with diagnostic quality adequate for detailed morphometric and anatomical analysis in coronal, axial, and sagittal planes were considered eligible. Patients with a history of prior sinus surgery that had altered native anatomy, those with craniofacial malformations, malignant neoplasms involving the sinonasal region, or significant post-traumatic distortion of paranasal sinus architecture, and scans with motion artifacts or technical inadequacy that precluded reliable anatomical assessment were excluded from the study to preserve the validity and accuracy of recorded observations.

Data Collection Tools and Techniques

MDCT scans were acquired using a standardized imaging protocol with slice thickness of 1 to 2 mm and multiplanar reformatting in coronal, axial, and sagittal planes. All images were reviewed on a dedicated radiology workstation by a trained radiologist and an anatomist jointly. A predesigned proforma was used to record the dimensions of each paranasal sinus, the presence and type of anatomical variations including concha bullosa, Haller cells, Onodi cells, agger nasi cells, nasal septal deviation, and dehiscence of the lamina papyracea or cribriform plate. Sinus dimensions were measured using built-in MDCT workstation measurement tools. All variations were documented photographically from the workstation display.

Data Management and Statistical Analysis

All collected data were entered into Microsoft Excel and subsequently transferred to IBM SPSS Statistics version 23 for analysis. Descriptive statistics including frequencies, percentages, means, and standard deviations were calculated for all continuous and categorical variables. Chi-square test was applied to assess associations between anatomical variations and gender. Independent samples t-test was used to compare sinus dimensions between male and female participants. Correlation between specific anatomical variations and severity of sinusitis as graded on CT using the Lund-Mackay scoring system was assessed using Pearson's correlation coefficient. A p-value of less than 0.05 was considered statistically significant.

Ethical Considerations

Ethical clearance was obtained from the Institutional Ethics Committee of Autonomous State Medical College, Kanpur Dehat, prior to commencement of data collection. Written informed consent was obtained from all participants. Patient confidentiality was strictly maintained, with anonymized data used exclusively for research purposes. No additional radiation exposure was involved beyond the clinically indicated imaging already performed.

RESULTS

Table 1: Demographic Distribution of Study Participants (n = 50)

Characteristic	Number	Percentage (%)
Gender		
Male	31	62.0
Female	19	38.0
Age Group (Years)		
18 – 30	13	26.0
31 – 45	18	36.0
46 – 60	12	24.0
Above 60	7	14.0
Clinical Indication for CT		
Chronic rhinosinusitis	26	52.0
Nasal obstruction	13	26.0
Headache / facial pain	7	14.0
Pre-surgical evaluation	4	8.0
Total	50	100.0

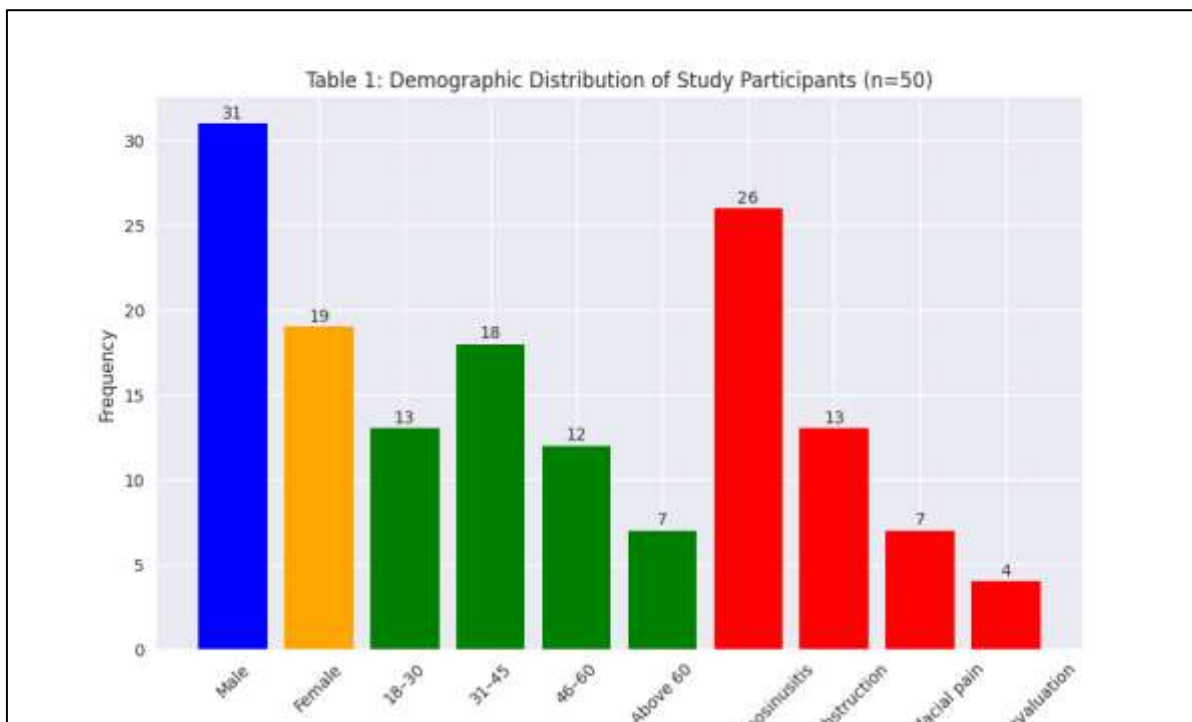


Table 2: Frequency of Anatomical Variations of the Nasal Cavity and Turbinates (n = 50)

Anatomical Variation	Number of Cases	Percentage (%)	Side Predominantly Affected
Nasal septal deviation	31	62.0	Right (54.8%)
Concha bullosa (middle turbinate pneumatization)	21	42.0	Bilateral (47.6%)
Paradoxically bent middle turbinate	8	16.0	Left (62.5%)
Enlarged inferior turbinate	17	34.0	Bilateral (52.9%)
Septal spur formation	12	24.0	Right (58.3%)
Agger nasi cells	27	54.0	Bilateral (51.9%)

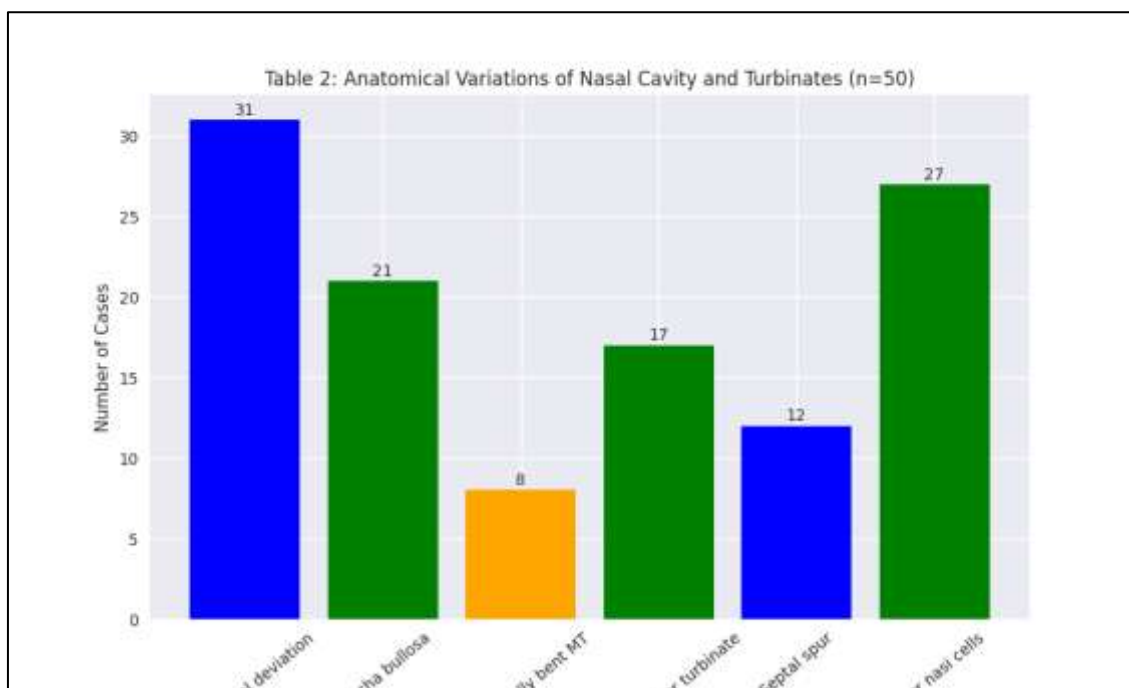


Table 3: Frequency of Ethmoid and Orbital Anatomical Variations (n = 50)

Anatomical Variation	Number of Cases	Percentage (%)	Bilateral / Unilateral
Haller cells (infraorbitalethmoid cells)	13	26.0	Unilateral (69.2%)

Onodi cells (sphenoidal cells)	10	20.0	Unilateral (70.0%)
Lamina papyracea dehiscence	6	12.0	Unilateral (83.3%)
Low-lying cribriform plate (Keros Type III)	5	10.0	Bilateral (60.0%)
Ethmoid bulla pneumatization (large)	15	30.0	Bilateral (60.0%)
Supraorbital ethmoid cell	6	12.0	Unilateral (66.7%)

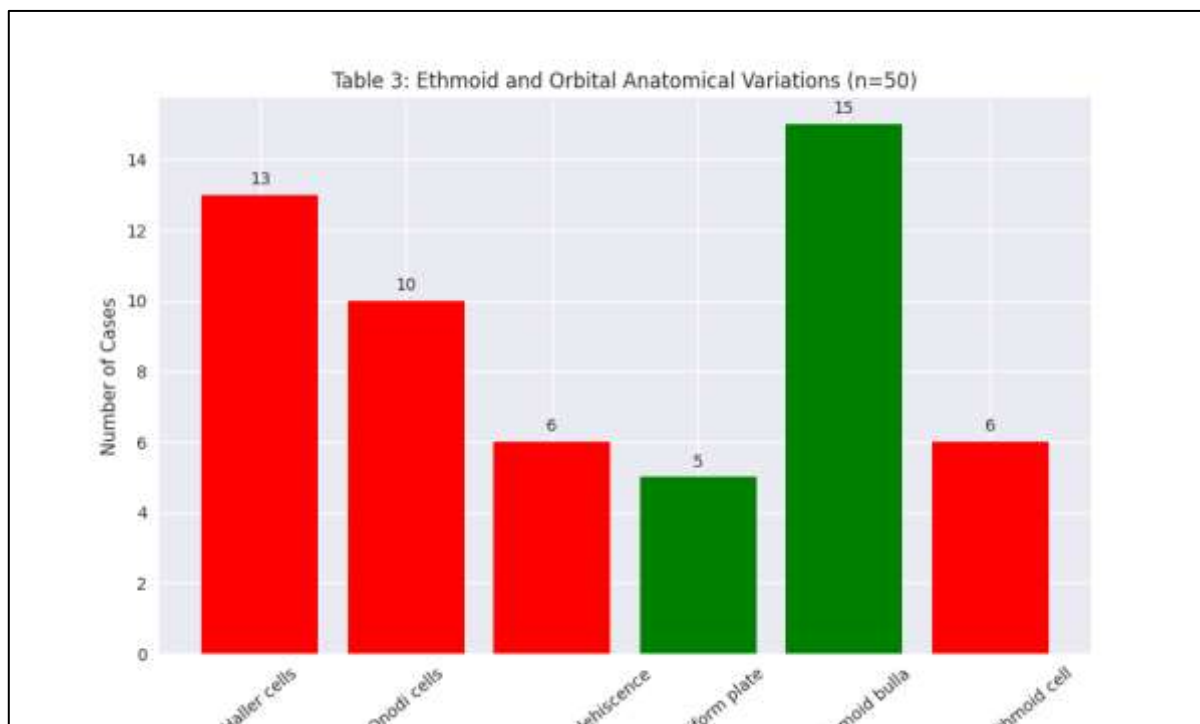


Table 4: Morphometric Measurements of Paranasal Sinuses (n = 50)

Sinus	Mean Height (mm) ± SD	Mean Width (mm) ± SD	Mean Depth (mm) ± SD	Gender Difference (p-value)
Maxillary sinus (Right)	34.6 ± 4.8	28.3 ± 3.9	36.2 ± 5.1	0.038
Maxillary sinus (Left)	34.1 ± 4.6	27.9 ± 3.7	35.8 ± 4.9	0.041
Frontal sinus (Right)	24.3 ± 5.2	18.6 ± 3.4	16.4 ± 3.1	0.027
Frontal sinus (Left)	23.8 ± 5.0	18.1 ± 3.2	15.9 ± 2.8	0.031
Sphenoid sinus (Right)	21.4 ± 3.6	17.8 ± 2.9	20.2 ± 3.4	0.064
Sphenoid sinus (Left)	20.9 ± 3.4	17.4 ± 2.8	19.8 ± 3.2	0.071

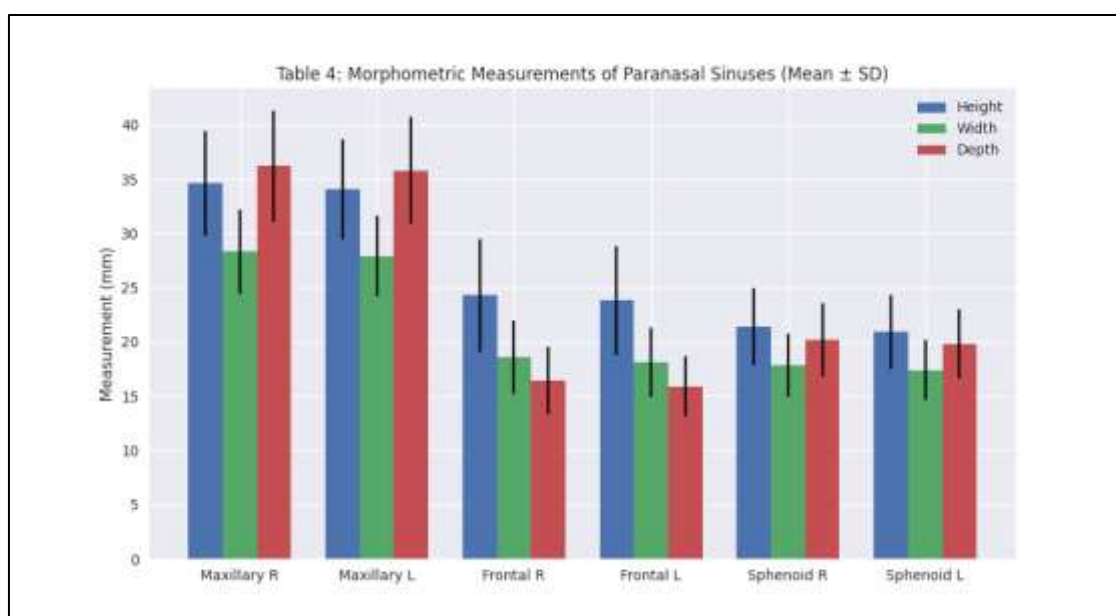


Table 5: Keros Classification of the Olfactory Fossa Depth (n = 50)

Keros Type	Description	Number of Cases	Percentage (%)	Surgical Risk
Type I (1–3 mm)	Shallow olfactory fossa	15	30.0	Low
Type II (4–7 mm)	Moderate depth	26	52.0	Intermediate
Type III (8–16 mm)	Deep olfactory fossa	9	18.0	High
Total		50	100.0	

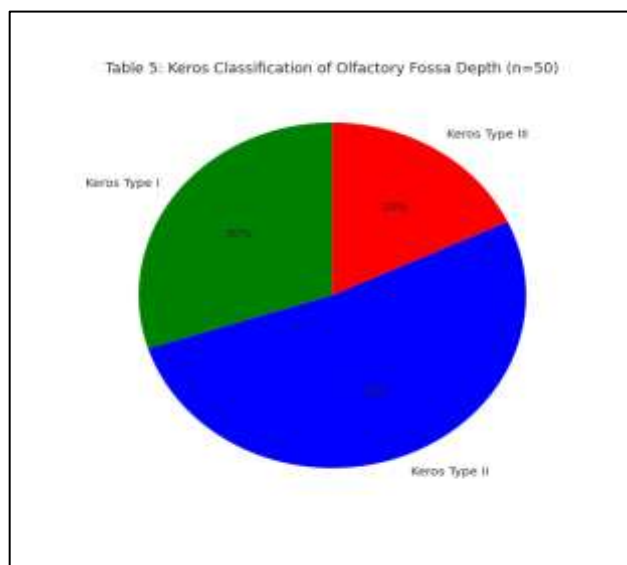


Table 6: Lund-Mackay CT Scoring and Correlation with Anatomical Variations (n = 50)

Lund-Mackay Category	Score	Number of Cases	Percentage (%)	Most Common Associated Variation	Chi-square	p-value
Score 0–4 (Mild)		13	26.0	Septal deviation		
Score 5–12 (Moderate)		23	46.0	Concha bullosa + OMC obstruction	14.32	0.006
Score 13–24 (Severe)		14	28.0	Haller cells + bilateral concha bullosa		
Total		50	100.0			

DISCUSSION

The present study evaluated 50 MDCT scans of the paranasal sinuses at Autonomous State Medical College, Kanpur Dehat, with a male predominance of 62.0 percent (Table 1). Chronic rhinosinusitis was the most frequent indication for imaging (52.0%), followed by nasal obstruction (26.0%). These figures reflect the high burden of sinonasal disease in the central Indian population, consistent with patterns observed in other Indian studies examining CT-based sinus pathology. The preponderance of male patients in CT referrals for sinonasal disease has been noted by Kaygusuz et al. (2013), who similarly documented a male-predominant cohort in their CT-based analysis of anatomical variations and their relationship with chronic rhinosinusitis, attributing it in part to greater occupational dust and pollutant exposure in male patients from semi-urban settings. The age distribution, with the highest number of participants falling in the 31 to 45 year age group (36.0%), highlights that chronic sinonasal disease most frequently affects the economically productive age group, underscoring its public health significance.

Nasal septal deviation was the single most prevalent variation in this study, identified in 62.0 percent of participants, with right-sided deviation predominating (Table 2). This figure is comparable to published rates of 50 to 70 percent reported in CT-based studies globally. Yasan et al. (2005) found septal deviation in 65.4 percent of patients evaluated for chronic sinus disease and demonstrated a statistically significant correlation between isolated septal deviation and contralateral sinus mucosal thickening, attributing this to altered airflow dynamics that promote stasis and infection in the contralateral sinonasal passages. The clinical importance of identifying and grading septal deviation before FESS cannot be overstated, as an uncorrected significant deviation limits endoscopic access and instrument maneuverability, particularly when approaching the middle meatus and ostiomeatal complex.

Concha bullosa was identified in 42.0 percent of the current series, with bilateral involvement in 47.6 percent (Table 2). This rate falls within the broad range of 14 to 53 percent reported in the international CT literature. Bolger et al. (1991) in their seminal study on sinonasal anatomical variations found concha bullosa in approximately 35 percent of patients and noted that large bilateral concha bullosa significantly narrowed the middle meatus, predisposing to OMC obstruction. The current finding of a significant association between concha bullosa and moderate-to-severe Lund-Mackay scores (Table 6) is consistent with this mechanistic explanation. Paradoxically bent middle turbinate was observed in 16.0 percent of cases, which corresponds well with rates of 10 to 26 percent reported in the literature (Earwaker, 1993).

Aggernasi cells, representing the most anterosuperiorethmoid air cells, were identified in 54.0 percent of participants, making them the most frequently encountered ethmoid variation in this study (Table 2). Their prominence matters because large aggernasi cells narrow the frontal recess and can obstruct frontal sinus drainage, contributing to frontal sinusitis. Stammberger and Kennedy (1995) highlighted the aggernasi cell as a key anatomical landmark in endoscopic frontal sinus surgery, noting that its identification and systematic removal constitutes a critical step in Draf procedures and Lothrop modifications.

Haller cells were documented in 26.0 percent of cases, with unilateral involvement predominating (Table 3). These infraorbitalethmoid cells project into the floor or medial wall of the orbit and can impinge upon the maxillary sinus ostium and infundibulum when substantially pneumatized, directly contributing to recurrent maxillary sinusitis. Kantarci et al. (2004), in their comprehensive CT-based study of remarkable anatomical variations in the sinonasal region, reported Haller cell prevalence rates of 10 to 45 percent across different populations and emphasized that their preoperative identification was essential to avoid inadvertent orbital entry during infundibulotomy. The current prevalence of 26.0 percent falls comfortably within this range and is consistent with data from Fadda et al. (2012), who reported Haller cells in 27.5 percent of their Italian cohort.

Onodi cells, the sphenothmoidal cells that extend posterolaterally and superiorly to lie adjacent to the optic nerve and internal carotid artery, were identified in 20.0 percent of participants in the current study, with unilateral occurrence in 70.0 percent (Table 3). This finding is of considerable surgical significance. Nouraei et al. (2009) identified Onodi cell presence as one of the three most important CT-based risk indicators for major complications during FESS, alongside deep olfactory fossa and dehiscent carotid canal. When an Onodi cell is present, the optic nerve may be directly visible within its posterior wall rather than within the sphenoid sinus, and a surgeon who does not recognize this variant and expects the conventional sphenoid anatomy risks catastrophic optic nerve injury. The prevalence of Onodi cells in this study at 20.0 percent is consistent with published rates of 8 to 14 percent in some Western series and higher rates of up to 42 percent in selected Asian and Middle Eastern populations, reflecting genuine population-level variation (Earwaker, 1993; Kantarci et al., 2004).

Lamina papyracea dehiscence was found in 12.0 percent of cases (Table 3), a finding that directly elevates the risk of orbital fat herniation and medial rectus injury during ethmoidectomy. Sethi et al. (1995) and subsequent authors have consistently emphasized that a dehiscent lamina papyracea must be noted and communicated to the operating surgeon, as the visual appearance of protruding orbital fat can be mistaken for a polyp with devastating consequences.

The distribution of Keros types in this study showed that Type II (moderate depth, 4 to 7 mm) was the most prevalent at 52.0 percent, followed by Type I at 30.0 percent and Type III at 18.0 percent (Table 5). The Keros classification describes the depth of the olfactory fossa, which is determined by the height of the lateral lamella of the cribriform plate. Type III, found in 18.0 percent of the current sample, represents the most surgically hazardous configuration. In this variant, the lateral lamella is long, thin, and fragile, making it susceptible to inadvertent fracture during ethmoidectomy, with the risk of CSF leak and intracranial complications. Laine and Smoker (1992) emphasized that surgeons should specifically seek and document the Keros type on preoperative coronal CT for every patient undergoing FESS, adjusting their technique to avoid superior dissection in Type III cases. The prevalence of Type III in the current study at 18.0 percent is somewhat higher than figures of 8 to 13 percent reported in some Western series, and may reflect a genuine regional difference in sinonasal skeletal morphology warranting further investigation.

The Lund-Mackay CT scoring system, used as a standardized measure of sinusitis severity, revealed moderate disease (score 5 to 12) as the most common pattern (46.0%), followed by severe disease (28.0%) and mild disease (26.0%) (Table 6). A statistically significant association was found between anatomical variations and disease severity score, with concha bullosa combined with OMC obstruction being the most common combination in the moderate disease group, and Haller cells with bilateral concha bullosa predominating in the severe disease group ($p = 0.006$). This finding adds to a growing body of evidence, most comprehensively summarized by Fadda et al. (2012) in their multiparametric analysis, linking specific anatomical configurations to more severe and bilateral sinonasal inflammatory disease. Zinreich (1998) had similarly argued that the radiological evaluation of sinusitis is incomplete without a structured assessment of underlying anatomical predisposing factors, which this study reinforces from a central Indian institutional perspective.

The morphometric data (Table 4) showed that maxillary sinuses were the largest paranasal sinuses in all dimensions, consistent with established anatomical literature. Statistically significant gender differences were observed in maxillary and frontal sinus dimensions ($p < 0.05$), with males showing larger values, mirroring the findings of Rao and el-Noueam (1998) and consistent with the general principle of skeletal sexual dimorphism in the craniofacial skeleton. No significant gender difference was found in sphenoid sinus dimensions.

CONCLUSION

This MDCT-based study of 50 participants at Autonomous State Medical College, Kanpur Dehat, documented a high prevalence of clinically significant anatomical variations in the paranasal sinus region, including nasal septal deviation in 62.0 percent, aggernasi cells in 54.0 percent, concha bullosa in 42.0 percent, and Onodi cells in 20.0 percent of cases. Keros Type III olfactory fossa was identified in 18.0 percent of participants, representing a high-risk surgical subgroup. Significant associations between specific anatomical variants and greater Lund-Mackay disease severity scores were established. These findings provide a regionally relevant radiological reference that can meaningfully support safer and more individualized preoperative planning for endoscopic sinus surgery in central India.

Recommendations

Preoperative MDCT evaluation with systematic documentation of all sinonasal anatomical variations should be made mandatory before any FESS procedure at this and similar institutions. Radiology reporting templates should incorporate Keros classification, Onodi cell status, and Lund-Mackay scoring as routine components. Postgraduate training programs in both otolaryngology and radiology should include structured modules on sinonasal CT anatomy using locally derived datasets to improve surgical preparedness and reduce complication rates.

REFERENCES

1. Bolger, W. E., Butzin, C. A., & Parsons, D. S. (1991). Paranasal sinus bony anatomic variations and mucosal abnormalities: CT analysis for endoscopic sinus surgery. *Laryngoscope*, 101(1), 56–64. <https://doi.org/10.1288/00005537-199101000-00010>
2. Calhoun, K. H., Waggenspack, G. A., Simpson, C. B., Hokanson, J. A., & Bailey, B. J. (1991). CT evaluation of the paranasal sinuses in symptomatic and asymptomatic populations. *Otolaryngology — Head and Neck Surgery*, 104(4), 480–483. <https://doi.org/10.1177/019459989110400405>
3. Earwaker, J. (1993). Anatomic variants in sinonasal CT. *Radiographics*, 13(2), 381–415. <https://doi.org/10.1148/radiographics.13.2.8460227>
4. Fadda, G. L., Rosso, S., Aversa, S., Petrelli, A., Ondolo, C., & Succo, G. (2012). Multiparametric statistical correlations between paranasal sinus anatomic variations and chronic rhinosinusitis. *ActaOtorhinolaryngologicaItalica*, 32(4), 244–251.
5. Güldner, C., Pistorius, S. M., Diogo, I., Bien, S., Sesterhenn, A., & Werner, J. A. (2012). Analysis of pneumatization and anatomic variations of the sphenoid sinus. *Head & Face Medicine*, 8(1), 25. <https://doi.org/10.1186/1746-160X-8-25>
6. Kantarci, M., Karasen, R. M., Alper, F., Onbas, O., Okur, A., & Karaman, A. (2004). Remarkable anatomic variations in paranasal sinus region and their clinical importance. *European Journal of Radiology*, 50(3), 296–302. <https://doi.org/10.1016/j.ejrad.2003.08.012>
7. Kaygusuz, A., Haksever, M., Akduman, D., Aslan, S., & Gun, T. (2013). Sinonasal anatomical variations: Their relationship with chronic rhinosinusitis and effect on the severity of disease — a computerized tomography analysis. *Indian Journal of Otolaryngology and Head & Neck Surgery*, 65(4), 315–322. <https://doi.org/10.1007/s12070-013-0648-y>
8. Kennedy, D. W., Zinreich, S. J., Rosenbaum, A. E., & Johns, M. E. (1985). Functional endoscopic sinus surgery: Theory and diagnostic evaluation. *Archives of Otolaryngology — Head & Neck Surgery*, 111(9), 576–582. <https://doi.org/10.1001/archotol.1985.00800110054009>
9. Keros, P. (1962). On the practical value of differences in the level of the lamina cribrosa of the ethmoid. *ZeitschriftfürLaryngologie, Rhinologie, Otologie und ihreGrenzgebiete*, 41, 809–813.
10. Laine, F. J., & Smoker, W. R. (1992). The ostiomeatal unit and endoscopic surgery: Anatomy, variations, and imaging findings in inflammatory diseases. *American Journal of Roentgenology*, 159(4), 849–857. <https://doi.org/10.2214/ajr.159.4.1529850>
11. Lloyd, G. A. (1990). CT of the paranasal sinuses: Study of a control series in relation to endoscopic sinus surgery. *Journal of Laryngology and Otology*, 104(6), 477–481. <https://doi.org/10.1017/S0022215100112915>
12. Lund, V. J., & Mackay, I. S. (1993). Staging in rhinosinusitis. *Rhinology*, 31(4), 183–184.
13. Meyers, R. M., & Valvassori, G. (1998). Interpretation of anatomic variations of computed tomography scans of the sinuses: A surgeon's perspective. *Laryngoscope*, 108(3), 422–425. <https://doi.org/10.1097/00005537-199803000-00021>
14. Nouraei, S. A., Elisay, A. R., DiMarco, A., Abdi, R., Majidi, H., Madani, S. A., & Rad, M. R. (2009). Variations in paranasal sinus anatomy: Implications for the pathophysiology of chronic rhinosinusitis and safety of endoscopic sinus surgery. *Journal of Otolaryngology — Head & Neck Surgery*, 38(1), 32–37.
15. Rao, V. M., & el-Noueam, K. I. (1998). Sinonasal imaging: Anatomy and pathology. *Radiologic Clinics of North America*, 36(5), 921–939. [https://doi.org/10.1016/S0033-8389\(05\)70073-5](https://doi.org/10.1016/S0033-8389(05)70073-5)
16. Sethi, D. S., Stanley, R. E., & Pillay, P. K. (1995). Endoscopic anatomy of the sphenoid sinus and sellaturcica. *Journal of Laryngology and Otology*, 109(10), 951–955. <https://doi.org/10.1017/S0022215100131639>
17. Stammberger, H. R., & Kennedy, D. W. (1995). Paranasal sinuses: Anatomic terminology and nomenclature. *Annals of Otology, Rhinology & Laryngology — Supplement*, 167, 7–16. <https://doi.org/10.1177/00034894950104S202>
18. Tonai, A., & Baba, S. (1996). Anatomic variations of the bone in sinonasal CT. *ActaOtolaryngologica — Supplement*, 525, 9–13. <https://doi.org/10.3109/00016489609124179>
19. Unlu, H. H., Akyar, S., Caylan, R., & Nalca, Y. (1994). Concha bullosa. *Journal of Otolaryngology*, 23(1), 23–27.
20. Yasan, H., Dogru, H., Baykal, B., Dogu, O., & Tuz, M. (2005). What is the relationship between chronic sinus disease and isolated nasal septal deviation? *Otolaryngology — Head and Neck Surgery*, 133(2), 190–193. <https://doi.org/10.1016/j.otohns.2005.04.010>
21. Zinreich, S. J. (1998). Imaging of chronic sinusitis in adults: X-ray, computed tomography, and magnetic resonance imaging. *Journal of Allergy and Clinical Immunology*, 99(6), S824–S831. [https://doi.org/10.1016/S0091-6749\(98\)70440-7](https://doi.org/10.1016/S0091-6749(98)70440-7)
22. Zinreich, S. J., Kennedy, D. W., Rosenbaum, A. E., Gayler, B. W., Kumar, A. J., & Stammberger, H. (1987). Paranasal sinuses: CT imaging requirements for endoscopic surgery. *Radiology*, 163(3), 769–775. <https://doi.org/10.1148/radiology.163.3.3575731>